Materials Science and Engineering B 154–155 (2008) 240–246

Contents lists available at ScienceDirect

Materials Science and Engineering B

journal homepage: www.elsevier.com/locate/mseb

Experimental investigations of boron diffusion mechanisms in crystalline and amorphous silicon

D. De Salvador[a,*], E. Napolitani[a], S. Mirabella[b], E. Bruno[b], G. Impellizzeri[b], G. Bisognin[a], E.F. Pecora[b], F. Priolo[b], A. Carnera[a]

[a] MATIS INFM-CNR and Dipartimento di Fisica, Università di Padova, via Marzolo 8, 35131 Padova, Italy
[b] MATIS INFM-CNR and Dipartimento di Fisica e Astronomia, Università di Catania, via S. Sofia 64, 95123 Catania, Italy

ARTICLE INFO

Article history:
Received 5 May 2008
Received in revised form 25 August 2008
Accepted 4 September 2008

Keywords:
Silicon
Diffusion
Doping

ABSTRACT

Boron, as the main p-type dopant in Si, has been extensively investigated both experimentally and theoretically in order to understand its diffusion mechanisms for modelling and optimization of advanced devices. Crystalline Si matrix was mostly studied, but quite recently increased interest emerged on the behaviour of B in amorphous Si. In this work we present our recent progress in understanding these fundamental processes. Extensive investigation about the room temperature diffusion of B induced by the analyzing beam during secondary ion mass spectrometry, allowed to give information about diffusion mechanism of B both in crystalline and in amorphous phase. Moreover this put the basis for accurate measurements that allowed to investigate the key parameters describing the B diffusion in different equilibrium conditions, i.e. in wide ranges of temperature and doping level. On this basis, a comprehensive, experimentally based, atomistic model for B diffusion has been assessed, advancing and clarifying in a coherent picture the wide existing literature, including the interactions among B and self-interstitial in different charge states. Also the amorphous phase shows a complex B diffusion mechanism, far from being Fick-like. By means of simulation modelling of extensive diffusion data, produced in a wide range of temperatures, times and B concentrations, we have demonstrated that B promotes the formation of dangling bonds and it interacts with them in order to diffuse. Peculiar physical features, such as diffusion shape and transient diffusion, are correctly described by the model.

1. Introduction

As it is known, miniaturization is fundamental for improving devices performances. Doping is one of the key physical processes in the micro and nano electronic field, allowing for spatial modulation of the semiconductor electrical properties. The current production technology sees the diffusion processes of dopants as crucial physical steps that has to be finely controlled in order to allow for dopant activation without profile sharpness deterioration. In the present paper we will review some fundamental aspects of B (the main p-dopant in Si) diffusion in both crystal and amorphous phases of Si. While the relevance of B diffusion in crystalline matrix is apparent by many decades, the relevance of B diffusion in amorphous phase is quite recently proposed due to the relatively recent use of pre-amorphization processes as a concrete alternative to direct ion implantation of dopants into crystalline Si (see reviews in Ref. [1] and the following references).

In general, we will show how diffusion mechanism of B is mediated by defects of the matrix in both amorphous (a-Si) and crystalline (c-Si) cases disclosing many atomistic details of such mechanisms. Mediated diffusion means that the B atom can only move after a close interaction with a defect inducing the formation of a mobile, metastable complex containing B. The interaction frequency is called g, while the means distance covered by the complex is called λ. g depends on the amount of defects and their diffusivity, while λ depends on the energy barriers regulating the movement and the stability of the complex. The macroscopic diffusivity parameter D is related to these two basic quantity by the equation: $D = g\lambda^2$ [2]. According to the physical processes regulating g and λ in different conditions, the shape assumed by very sharp doped profiles (delta-doping) after diffusion can strongly deviate from a pure Fick-like diffusion. This is what happens both in a-Si and c-Si, allowing for an experimental investigation of the detailed atomistic mechanisms through proper modeling of concentration profiles of samples produced in different controlled experimental conditions.

In particular, a large number of papers state that self-interstitials (Is) mediate the diffusion in c-Si [2–6]. The BI complex formed after

* Corresponding author. Tel.: +39 0498 277004; fax: +39 0498 277000.
E-mail address: desalvador@padova.infm.it (D. De Salvador).

0921-5107/$ – see front matter © 2008 Elsevier B.V. All rights reserved.
doi:10.1016/j.mseb.2008.09.010

interaction travels for relatively long λ before thermally breaking or being captured by an impurity. This fact strongly characterizes the tails of delta-doping diffusion allowing for g and λ independent measurement. We have measured the above parameters both at room temperature (RT), when Is are provided by secondary mass spectrometry sputtering beam [7] and at relatively high temperatures under different doping conditions, i.e. when I are thermally generated [8]. These data allowed to asses the reactions among I, B (and their charge states) and free charges governing the B diffusion mechanism. We show that the interactions with neutral I^0 and double positively charged I^{2+} are the main channels for B diffusion. The BI^- and BI^+ complexes formed by these interactions switch to BI^0 before diffusing [8]. These results allowed to solve a 30 years long debate on B diffusion mechanism and have been recently confirmed by Bracht and coworkers by an independent methodology that simultaneously investigates the Si self diffusion, by isotope tracing, and B diffusion [9].

Despite the advanced comprehension of B diffusion mechanism in c-Si, the counterpart in a-Si has been almost totally neglected. In fact, only very recently this research field is being attracting both scientific and technologic interest, and the first evidences of B diffusion [10,11] and clustering [12,13] in the amorphous phase have been provided.

Our investigations, which will be reported in the following, show that in a-Si there is no evidence of a long and measurable mean free path λ for B. The indirect mechanism of diffusion is suggested in this case by the transient character of diffusion and by a strong concentration dependent diffusion. Both these aspects are experimentally investigated and explained by a model that we have recently proposed in Ref. [14], according to which B diffusion is induced by dangling bond defects [15–17] of the amorphous phase.

In the following, in order to provide a general picture of B-Si mass transport interactions in crystalline and amorphous phases, our recent results on these hot-topics will be reviewed and compared.

2. Experimental

In order to study the B diffusion in c- and a-Si, very sharp B profiles were obtained by molecular beam epitaxy (MBE) growth and then measured by secondary ion mass spectrometry (SIMS). Details about growth protocol are reported elsewhere [7,19].

The B profiles have been characterized by SIMS with a non conventional approach, i.e. by controlling the sample temperature during sputtering. In this way, very interesting phenomena regarding B diffusion at room temperature are accessible. At the same time an unprecedented accuracy is reached for B detection in c-Si by combining the suppression of the sputtering induced diffusion phenomena, obtained by freezing the sample at −70 °C, with the enhancement of the B detection yield, obtained by flooding the sample with a jet of O_2 gas. Details about SIMS protocol are reported in Refs. [7,18].

The above protocol was used to characterize B diffusion in c-Si at high temperatures in equilibrium conditions with unprecedented accuracy (i.e. by eliminating the interaction with the beam) [8]. In order to perform this experiment the plan depicted in Fig. 1 was carried out. The basic idea is to analyze the diffusion of a sharp ^{11}B delta doping, determining the microscopic diffusion parameters (D, g and λ) while varying the background doping around the delta. The samples were grown by inserting a B spike at the depth of 180 nm, using a natural isotopic abundance solid B source, and a $Si_{1-x}C_x$ alloy layer (x = 0.3 at.%) between 390 and 440 nm. The structure was amorphized down to a depth of 500 nm by implanting Si ions (3×10^{15} ions/cm^2 at 250 keV plus 2×10^{15} ions/cm^2 at 40 keV, at the liquid nitrogen temperature) and afterwards, multiple ^{10}B

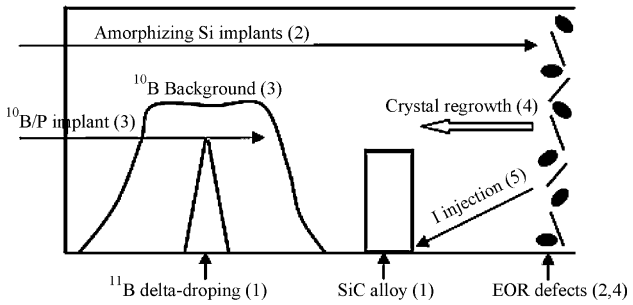

Fig. 1. B diffusion in c-Si: experiment plan. (1) Epitaxial growth of silicon with delta-doped B and a $Si_{1-x}C_x$ alloy barrier. (2) Amorphizing Si implants. (3) Multiple ^{10}B (or ^{31}P) implants to insert a B (or P) background around delta-doped B. (4) Solid phase epitaxial re-growth. (5) Diffusion annealing.

(or ^{31}P) implants were performed to produce the background doped box in the range between 110 and 250 nm. Background p-doping varied in the range 5×10^{18}–7.5×10^{19} cm^{-3} in the case of ^{10}B. For example, we implanted 3.42×10^{14} B/cm^2 at 26 keV, plus 4.56×10^{14} B/cm^2 at 43 keV, plus 10.05×10^{14} B/cm^2 at 68 keV to obtain the background box with a concentration of 7.5×10^{19} B/cm^3 while the other concentrations are obtained by rescaling the doses. A similar background of 3×10^{18} cm^{-3} was obtained in the case of ^{31}P by means of 1.95×10^{13} P/cm^2 at 70 keV, plus 1.5×10^{13} P/cm^2 at 120 keV, plus 4.95×10^{13} P/cm^2 at 175 keV ion implantation. Subsequent rapid thermal annealing (RTA) at 700 °C was performed in inert N_2 atmosphere to induce the re-crystallization of the amorphous phase (solid phase epitaxy, SPE) with an annealing of 15 s for p-doped samples and 10 min for the n-doped specimen.

Further thermal treatments at the 700 °C were than performed in order to induce diffusion of the previous starting samples. In particular the n-doped specimen was annealed for 14 and 32 h, two peaces of a sample without background undergoes 5 h and 18 h annealings, three 5×10^{18} B/cm^3 samples were annealed for 30 min, 1 and 2 h, 2.5×10^{19} B/cm^3 background samples had 10 and 20 min annealings, 5×10^{19} B/cm^3 background samples were annealed for 5 and 10 minutes and, finally, 7. 5×10^{19} B/cm^3 samples were annealed for 100 s, 200 s and 10 min. The Is injection from the residual damage below the amorphization depth (end of range defects) is screened by the $Si_{1-x}C_x$ alloy layer [19].

We verified that the amount of substitutional C in our samples is enough to avoid any Is supersaturation, since about 90% of C is still in substitutional sites even after the longest annealing. This was measured by nuclear reaction analysis and high resolution X-ray diffraction. By the same ways we also verified that B and P backgrounds are fully substitutional both before and after the annealings.

As far as the B diffusion in a-Si is concerned, the following experimental plan was followed, as described in Fig. 2. To better

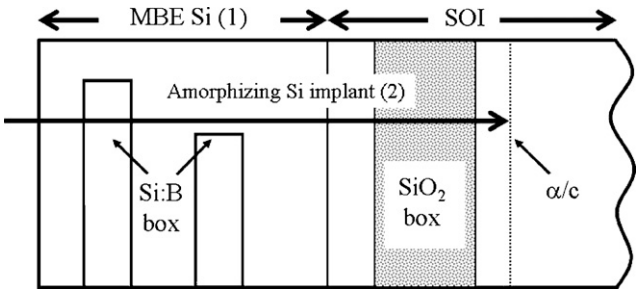

Fig. 2. B diffusion in a-Si: experiment plan. (1) Epitaxial growth of silicon with two, narrow B doped region upon a SOI substrate. (2) Amorphizing Si implants. (3) Diffusion annealing.

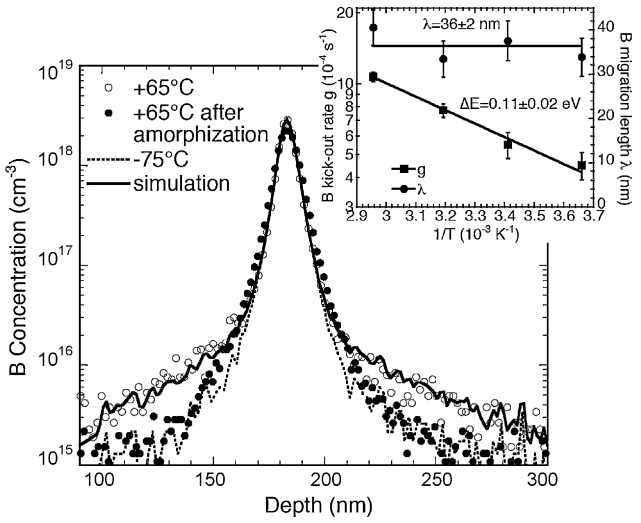

Fig. 3. SIMS profiles of a B delta in crystalline matrix performed at −75 °C (dashed line) and after sputtering for 80 nm at +65 °C (open circles). The continuous line is a simulation of this last profile. B delta measured at +65 °C after amorphization is shown with closed circles. The inset plots g and λ as a function of the inverse temperature.

investigate the phenomenon, B doped regions have to remain in the amorphous state as much as possible. Therefore, we used the silicon on insulator (SOI) approach [11] combined with the MBE growth. On a SOI substrate, we grew by MBE a 350 nm-thick Si layer with embedded two 20 nm thick B-doped regions at concentrations of 7×10^{19} and 8×10^{20} B/cm^3 (hereafter named as low- or high-B box, respectively) [14]. The structure was amorphized, by implanting Si ions, down to about 1 μm, i.e. well below the oxide layer acting as a barrier for any SPE re-growth starting from the original a/c interface. Thermal annealing in the 450–650 °C range were performed to induce the B diffusion in a-Si for times shorter than the onset of the random nucleation and growth phenomenon [14].

3. Results

3.1. Room temperature B migration in crystalline Si induced by SIMS

SIMS is the main tool to measure with a very good depth resolution dopant concentration profiles in a very wide range of concentrations and therefore it is fundamental for the present investigations. In a first set of experiments we investigated the reliability of such tool discovering very interesting effects that allowed for a strong improvement of the technique, and at the same time giving basic information on the diffusion mechanism in c-Si. Moreover, the experiment provided some initial indication about the issue of B diffusion in a-Si.

SIMS measurements (not shown here) of a B delta performed with sample at different temperatures from +65 °C to −75 °C showed marked differences with long tails progressively reducing by decreasing the temperature and disappearing below −50 °C [7]. In Fig. 3 we report an example of the above phenomenon, were a measurement was obtained at −75 °C (dashed line) and another one after having sputtered the samples at +65° for 80 nm (open circles), and concluding the measurement at −75 °C. The tails measured in the second measurements are the results of the interaction between the self-interstitials injected during sputtering at +65 °C and the B in the delta. As previously told, I and B interaction produce the BI complex that migrates for a mean free path λ, and the above results demonstrate that this occurs even at temperatures as low as RT.

Fitting of the data according to diffusion equation described in of Refs. [3,7,8] (continuous line in Fig. 3) allows extracting g and λ at different sputtering temperatures (Fig. 3, inset). As can be noted λ is clearly temperature independent, with a constant value of about 36 nm. This is due to the fact that in this case the BI mobile complex is not stopped in its migration by BI thermal breaking but by trapping at impurities that is constant with temperature [7]. The migration frequency g exhibits instead (Fig. 2) a clear exponential decrease with $1/T$ with a thermal activation energy of about 0.1 eV and can be interpreted as a small barrier for B–I interaction that can be evidenced at these low temperatures. Of course this barrier is very much lower than the barrier that has to be overcome to produce interstitial by thermal activation that is about 3–4 eV. Such a difference is due to the fact that in this situation the energy for producing I is not due to thermal vibrations but is given by the beam damaging.

A further interesting information about this experiment is reported in Fig. 3. Close circles represent the SIMS measurements performed at +65 °C on the same delta after a complete amorphization of the layer therefore by completely changing the Si matrix phase.

As can be noted the measurement does not present any significant SIMS induced B diffusion perturbation, giving a first indication that diffusion mechanism is very different in the two phases. Moreover, we will see that B diffusion under thermal equilibrium is much higher in a-Si than in c-Si that is exactly the opposite behaviour with respect to ion beam induced diffusion presented in this paragraph. This contradictory behaviour will be explained on the basis of the different physical models regulating diffusion in amorphous and crystalline phases.

3.2. Thermally induced B diffusion in c-Si

Thanks to the previous study, very accurate determination of λ can be obtained (down to 0.5 nm) allowing for detailed diffusion study even at high temperature where λ is strongly reduced by the thermal breaking of the BI pair.

We report the results of our study regarding the migration mechanism of B in c-Si with different Fermi level position. As described in the experimental section, we varied the hole concentration by two orders of magnitude by performing diffusion experiment of deltas in different backgrounds and extracted the values of D, g and λ by means of fitting procedure.

In Fig. 4 we show two examples of ^{11}B profiles for the 5×10^{18} at/cm^3 (circles) and 7.5×10^{19} at/cm^3 (triangles) ^{10}B background after diffusion for 1 h and 200 s respectively. The two profiles present quite different shapes: looking at the two side regions of the spikes in the 160–175 nm and 190–205 nm depth ranges, the first profile present exponential trends (linear in log-scale) characteristic of BI mediated diffusion with a long BI mean free path, while the second profile has a gaussian (parabolic in log-scale) shape characteristic of a Fick diffusion or of a small mean free path. The lines are the best fits to the diffused data obtained by numerically "diffusing" the as-regrown profile according to the equations of Ref. [2].

The D, g and λ values extracted for the different doping conditions and averaged over different annealing times are plotted in Fig. 5 as a function of the hole concentration p normalized by the intrinsic hole concentration in an undoped Si (n_i, equal to 0.92×10^{18} cm^{-3} at the diffusion temperature of 700 °C [20]). p is calculated starting from the background B concentration according to Boltzmann statistics and considering a full ionization of substitutional B. The whole set of D, g and λ furnishes very detailed

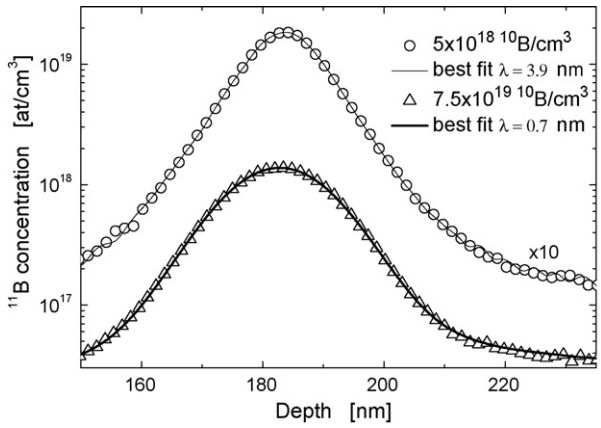

Fig. 4. SIMS measurements of concentration profiles of ^{11}B spike after diffusion annealing for samples with a 5×10^{18} at/cm^3 (circles) and a 7.5×10^{19} at/cm^3 (triangles) ^{10}B background. The lines are the best fits to the data obtained with $\lambda = 3.9$ nm and $\lambda = 0.7$ nm, respectively. Data and simulation relative to 5×10^{18} at/cm^3 sample are multiplied by a factor 10 for the sake of clarity.

information on the B diffusion mechanism under different Fermi level positions.

The trend of D is very well fitted by a linear function in the whole range [$D = D_0(p/n_i)$], extending the assessed trend proposed in the literature [21] to lower temperatures. Such a trend is univocally related to the charge state of the mobile BI complex since it indicates that the whole diffusion process proceeds by the net exchange of a single positive charge (whose density increases linearly with p/n_i).

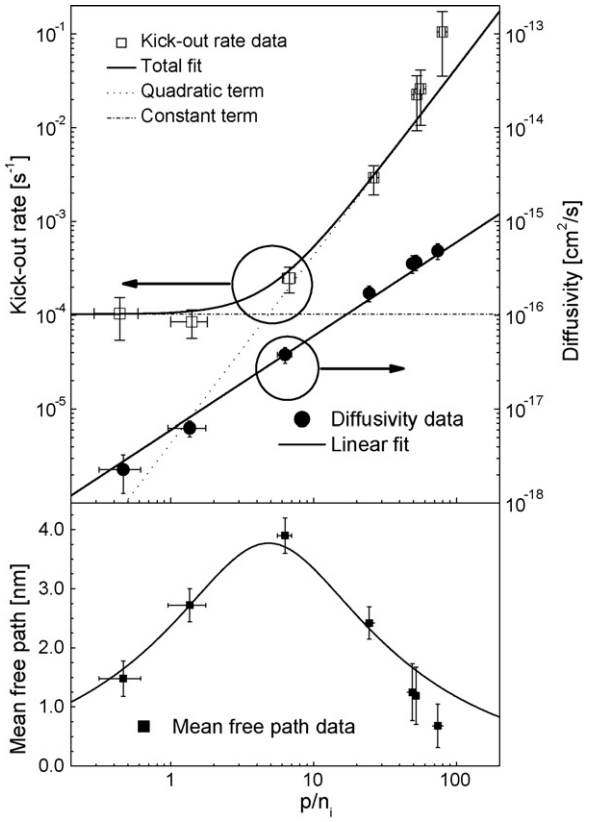

Fig. 5. Experimental data on diffusivity (closed circles), kick-out rate (open squares) and mean free path (closed squares) as a function of the hole excess introduced by the doping background (p/n_i). The continuous lines are the best fits to the data, while dotted (dashed) line is the quadratic (constant) dependence of the kick-out rate over the doping background.

A substitutional B atom (B_S), which is singly negatively charged before diffusion starts, has to interact with one I and get one hole to form the BI^0 complex able to diffuse.

The g and λ trends deeper explain the migration paths involved at different Fermi level position. The g trend has two components as a function of the hole density: a constant one and a quadratic one. This can be thought as if the interaction with I, that promotes the formation of the BI complex, is driven by neutral I (I^0) or by a doubly positive I (I^{2+}). The populations of such species have a constant and a quadratic trend with p/n_i [8], thus introducing a constant g_0 and a quadratic $g_{2+}(p/n_i)^2$ term in the kickout frequency trend versus p/n_i: $g = g_0 + g_{2+}(p/n_i)^2$. As a consequence of this, at low or high p/n_i values BI complexes in negative or positive charge states are produced, respectively, according to the following reactions:

$$B_S^- + I^0 \rightarrow BI^-, \quad \text{or} \quad B_S^- + I^{2+} \rightarrow BI^+. \tag{1}$$

Both these two BI complexes are not the diffusing species as demonstrated by the D trend analysis, but they have to transform into BI^0 by changing their charge state before B diffusion, through a free carrier exchange. The λ trend clarifies the picture, since it represents the free mean path of the diffusing species. The bell shape traced by λ as a function of p/n_i is a consequence of the charge exchange that must occur to transform the BI$^-$ and BI$^+$ species into the mobile BI^0 species. When p/n_i is lower than 4, BI$^-$ is produced at first, and it has to get an hole to move, so BI mean free path increases by increasing the hole availability (i.e. by increasing p/n_i). On the contrary when p/n_i is larger than 4, BI$^+$ is produced, and it has to lose a hole to move. The higher is p, the lower is the probability that the latter reaction occurs, thus reducing the BI free mean path λ.

The data so far presented clarify the B diffusion mechanism in c-Si as a function of the Fermi level position. It has been consolidated that the main diffusing species is the BI^0 complex, which does not follow a simple interaction between B_S^- and I$^+$. Instead, preferential interactions of B_S^- with I^0 or with I^{2+} have been evidenced at low or high hole densities, respectively, followed by charge exchange towards the formation of the diffusing BI^0 complex.

3.3. B diffusion in amorphous Si

In the following the mechanism of B diffusion in a-Si will be investigated. The main features of such a diffusion are given in Fig. 6. The starting profile is related to the sample just after the amorphizing implant (circles), while the diffused one has been obtained after thermal annealing at 650 °C, 250 s (squares). Lines are simulations of the data that will be commented in the following.

B diffusion appears to be much higher in a-Si than in c-Si, where the mean diffusion length after similar thermal budgets would be negligible (from 10^{-2} to 10^{-3} nm [21]). There is a clear evidence of B clustering above about 2×10^{20} B/cm^3, as indicated by the kink in the high B box profile (see the arrow). The clustering evidence has been noted as soon as B diffusion is detectable and up to the longest time used at all temperatures, suggesting that B precipitation in a-Si occurs through quick formation of a B complex, in agreement with our recent results [12,13] and theoretical predictions [22]. On the other hand, the observed B profile broadening does not obey a standard Fick's law with constant and homogeneous diffusivity (D_B), since after annealing the concentration gradient significantly increases. Both B profiles assume a "box-like" shape with wide shoulders and narrow tails, which appears to be an opposite effect with respect to the tailing effect detected in c-Si. This fact is typical of diffusion phenomena where the diffusivity increases by increasing the diffusing species concentration. On the other hand, simulation trials with an univocal relation between B concentration and B diffusion (not shown) miss to describe a second important phenomenon, i.e. the significant difference in the

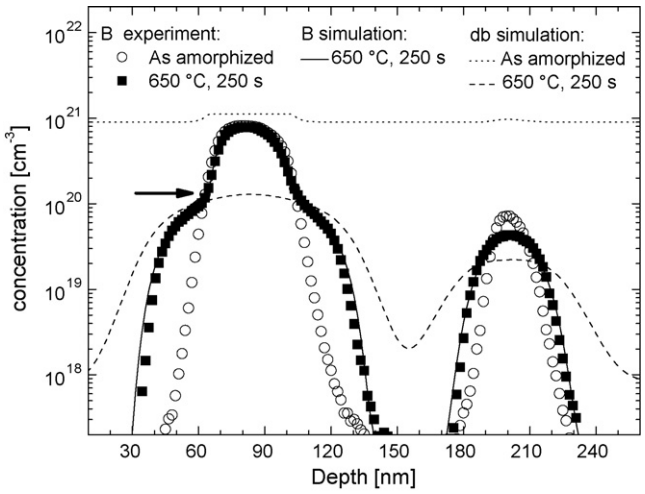

Fig. 6. B diffusion in amorphous Si. SIMS measurements of B concentration profiles in the as-amorphized sample (circles) and after annealing 650 °C, 250 s (squares). Best fit results (solid lines) are also shown. Continuous line is the simulation of B profile after diffusion. Dashed lines are the db concentration before and after annealing.

broadening of the two boxes, the high B box showing a larger diffusion than the low B for a fixed B concentration. In such a manner, B diffusivity seems to feel the global amount of B present in the surroundings, being higher in the high B box.

A third fundamental feature of the a-Si B diffusion is its transient nature that is clearly shown in Fig. 7. An effective B diffusivity (D_{eff}) for all the data is calculated, for the two boxes (high box: square, low box: circles), as the difference between the squared variance (σ^2) of the diffused B distribution with respect to the as-amorphized case ($\sigma^2{}_0$), divided by twice the annealing time (t): $D_{\text{eff}} = (\sigma^2 - \sigma^2{}_0)/2t$. Finally it is plotted versus annealing time for different temperatures in Fig. 7.

Under a standard Fick's law diffusion process, the so calculated effective B diffusivity should be constant and homogeneous, while our data show a transient and concentration dependent B diffusivity. D_{eff} is systematically higher in the high B box, and an evident decrease of D_{eff} is observed in all the cases, for both the boxes, within a quite wide time scale. In order to explain these features we could invoke an indirect diffusion for B in a-Si, mediated by some defects present in the amorphous phase. It is well known that during annealing, a-Si relaxes reducing the defect density and thus affecting the B diffusion, if mediated by such defects. Still, at all temperatures, the a-Si relaxation time reported in literature [Ref. 23 and references therein] is well shorter (10–100 times) than the observed diffusivity transient. Thus, a not trivial hypothesis has to be found, accounting for the concentration dependence and the relatively long transient diffusion time.

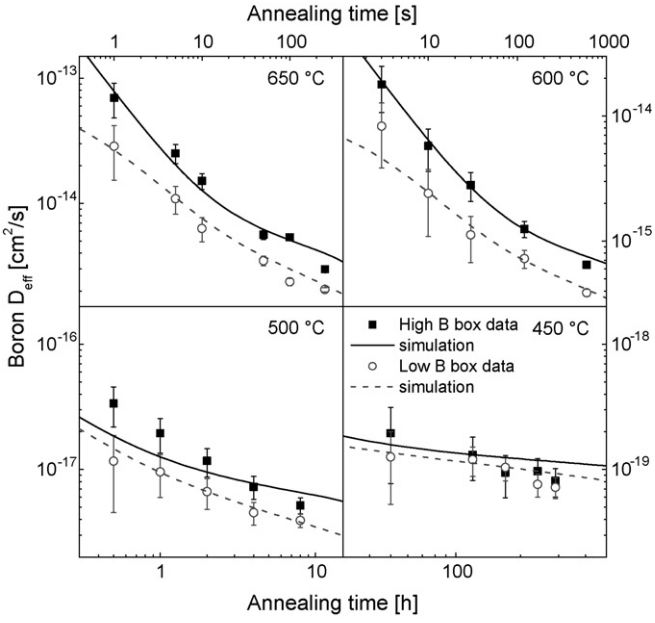

Fig. 7. Time evolution of the effective B diffusivity in amorphous Si extracted from the high (squares) and the low (circles) B boxes for all the annealing processes. Simulations of D_{eff} (lines) are also shown.

The effect of the defect density modification during thermal relaxation has been investigated into deeper details by the following test. During the annealing at 650 °C for 100 s, we de-relaxed the sample (breaking the thermal process after the first 50 s) by implanting Ge ions (300 keV, 6×10^{13} /cm^2, corresponding to 0.1 displacements per atom). This Ge implantation raises up the defect density as in the un-relaxed state [16], not affecting the B profile. The B profile of this sample (not shown) is almost undistinguishable from that of a sample annealed for 100 s at the same temperature without the de-relaxation implant. Thus, we could say that the defect annihilation during the relaxation have a minor role on B diffusion.

This fact does not mean that there is not a relation between amorphous defects and B diffusion, on the contrary, all the features up to now described can be taken into account by exploiting a diffusion mediated model in which dangling bonds (db) mediate the diffusion of B.

By means of Cu decoration techniques, described in Ref. [24], we observed that B doped a-Si layers are richer in defects than undoped matrices, both in the unrelaxed and in the relaxed state. Similarly, Muller et al. [25] have observed that in thermally relaxed a-Si, impurities are usually incorporated within a 3-fold coordination site and a large kinetic barrier exists against the conversion to the tetrahedral site. Thus, it is very reasonable that B atom, 4-fold coordinated in c-Si, upon amorphization is accommodated into a 3-fold coordinated site, breaking one Si–B bond and generating an excess of db in the network.

Therefore, to model the collected data we assumed that B migration in a-Si occurs via a boron jump between adjacent 3-fold coordination sites through the temporary restoring of a metastable, 4-fold coordinated B, by the capture and release of 1 db, as follows:

$$B_3 + db \leftrightarrow B_4. \quad (2)$$

The time evolution of the B profile has to be modelled in conjunction with the time evolution of the db population, whose density is transiently increased just after ion implantation or permanently enhanced by the presence of the boron atoms themselves. This model, whose details and rate equations are presented in Ref. [14], accounts for the transient and concentration dependence of B diffusion. The continuous lines in 6 and 7 are best fits to the data obtained following this model.

The non Fick-like diffusion is explained considering that the higher the B density, the more db are present, promoting a faster B diffusion. The excess of db is higher in the higher doped regions, accounting for the wider broadening in the high B box. The transient diffusion is related both to the db–fb annihilation (for the very early stages of annealing and for de-relaxation case) and to the progressive reduction of db density due to db diffusion away from the B doped region.

As an example in Fig. 6 the optimized db concentration profile in the as amorphized starting profile (short dashed line) and after 250 s 650 °C annealing (long dashed line) are reported. As can be noted dbs concentration at the starting time is given by a constant

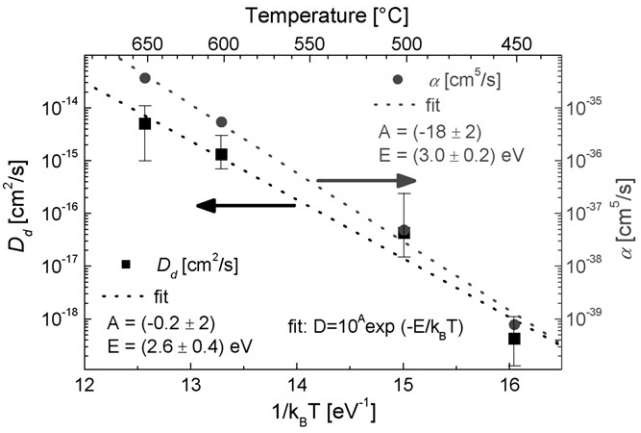

Fig. 8. Arrhenius plots for the diffusivities of dangling bonds (D_d, left axis) and of B per unit dangling bond density (α, right axis) in a-Si. Arrhenius fits (dotted lines) and results are also shown.

background of about 9×10^{20} cm^{-3} due to the ion beam induced dbs fbs excess plus a contribution due to B generation of dbs. After annealing, the dbs profile lowers causing the reduction of B diffusion. Even if the most part of the lowering is due to the fb–db annihilation after which only the B induced dbs excess survive, the B diffusion transient is regulated by the dbs out-diffusion from the initial B rich region. This last phenomenon takes a much longer time than annihilation to occur and is fundamental to obtain the good fit of transient data of Fig. 7. Moreover, according to the model, the B diffusion during db-fb annihilation is only a very minor part of the total diffusion since of its very short duration, explaining why the de-relaxation implant induce an almost negligible diffusion excess.

Both db and B diffusivities can be extracted within this model, spanning over six orders of magnitude and showing activation energies of 2.6 ± 0.4 and 3.0 ± 0.2 eV, respectively (see Fig. 8). B diffusivity (α) is intended per unit dangling bond density. These activation energies are very similar, meaning that B migration barrier is approximately fixed by db diffusion barrier.

The above energies are higher than B diffusion activation energies proposed in Ref. [11] that was about 2 eV. Such difference may be due to a difference in the data analysis, in fact in that paper diffusivity values for every time and temperature of annealing are reported but there is no specification about the model used to determine those values. Moreover we speculate that the great proximity to the surface of the B profile (about 10 nm) may strongly influence the diffusion dynamic introducing further parameters that are not needed to explain our "bulk" experiment. This last aspect should be further investigated in order to obtain predictive modelling of shallow B profiles before re-crystallization.

In summary, the proposed data and modelling explain the B diffusion mechanism in a-Si as an indirect migration mediated by db defect. B diffusivity in a-Si is some orders of magnitude higher than in c-Si, and present a transient character which can not be ascribed to the well-known a-Si relaxation alone.

4. Discussion

Some general comment about the a-Si and c-Si thermal diffusion can be now mentioned. As stated in the introduction a general description of defect mediated diffusion can be divided into 2 terms, λ and g. The first term depends on thermal stability and diffusivity of the mobile complex and was deeply investigated for c-Si in the first part of the paper. It strongly depends on temperature and on doping conditions and may assumes values as large as tens of nm. In the a-Si case, λ is very small, i.e. below the experimental sensitivity, for all the investigated temperatures, since simulation attempts (not shown) confirmed that the migrating species have a migration length well below 2 nm.

This fact is apparently contradictory with the much higher B diffusivity in a-Si with respect to c-Si. Evidently such trend should be mainly ascribed to g parameter. Such parameter depends on both how many defects are present in the sample and how much fast they can diffuse.

On one hand, in a-Si, the diffusivity of dbs has been shown to have an activation energy of more than 2 eV (see Fig. 8) while for Is diffusion in c-Si the energy barrier is around 1 eV [26]. On the other hand, in a-Si the dbs density has been shown to be very high and substantially supported by the B itself, while in c-Si the I concentration has a well high energetic barrier around 4 eV and therefore a very low concentration [26]. As a consequence, the higher B thermal diffusivity in a-Si can be explained considering that the density of the diffusion-mediator species is well higher than the corresponding one in c-Si.

This reasoning is coherent with the evidences reported for the room temperature SIMS-mediated diffusion experiment. Those data showed that the beam induced diffusion is only present in the crystalline phase and not in the amorphous phase, i.e. contrary to before, in these conditions we observed a much lower B diffusion in a-Si with respect to c-Si.

Very reasonably the reason for this is not due to the absence of defect formation in a-Si during sputtering (very likely the SIMS primary beam produce a lot of db defects in amorphous phase), instead it should be ascribed to the high db diffusion barrier (2.6 eV) that forbids any db migration around room temperature and therefore does not permit the formation of any mobile B complex.

5. Conclusions

The microscopic mechanism of B diffusion in crystalline and in amorphous Si has been experimentally fixed and justified by appropriate modeling. In both the Si matrixes, B migrates by the mediation of point defects in different and peculiar fashion.

B migrates within c-Si mainly via a neutral BI complex, whose formation depends on the Fermi level. For moderate p-type doping, B_S interacts preferentially with I^0 while at high p-type doping the same impurity couples with I^{2+}. In both cases, a free charge exchange between the BI complex and the hosting matrix is needed to have B diffusion, leading to the formation of the diffusing BI^0 complex.

B diffusion in a-Si has been also investigated, showing that it is an indirect event too. The diffusion of B in a-Si is shown to have a transient and concentration dependent behaviour. Moreover, it has been shown that the presence of B itself enhances the density of dangling bond in the matrix, since boron is incorporated in 3-fold coordinated sites. Finally, boron atoms are modelled to diffuse after the interaction with dangling bonds promoting the formation of a temporary and metastable, 4-fold coordinated B.

A comparison between the two mechanisms was described both in the SIMS-induced room temperature diffusion and thermal diffusion regimes.

Acknowledgments

The authors wish to thank C. Percolla, S. Tatì (CNR-INFM MATIS), A. Marino (CNR-IMM), R. Storti (University of Padova) for technical contribution, M. Mastromatteo, and M. Pesce (University of Padova) for useful discussions and experimental contribution.

References

[1] P. Pichler, Intrinsic point defects, impurities, and their diffusion in silicon, in: S. Selberherr (Ed.) (Springer, Wien-NewYork, 2004); L. Pelaz, L.A. Marquez, J. Barbolla, J. Appl. Phys. 96 (2004) 5948.
[2] N.E.B. Cowern, K.T.F. Janssen, G.F.A. van de Walle, D.J. Gravesteijn, Phys. Rev. Lett. 65 (1990) 2434;
N.E.B. Cowern, G.F.A. vandeWalle, D.J. Gravesteijn, C.J. Vriezema, Phys. Rev. Lett. 67 (1991) 212.
[3] J.W. Corbett, S. Mahayan, in: U. Goesele, T.Y. Tan (Eds.), Defects in Semiconductors II, North-Holland, New York, 1983, p. 45.
[4] J. Zhu, T. Diaz de la Rubia, L.H. Yang, C. Mailhiot, G.H. Gilmer, Phys. Rev. B 54 (1996) 4741.
[5] B. Sadigh, T.J. Lenosky, S.K. Theiss, M.J. Caturla, T. Diaz de la Rubia, A.M. Foad, Phys. Rev. Lett. 83 (1999) 4341.
[6] W. Windl, M.M. Bunea, R. Stumpf, S.T. Dunham, M.P. Masquelier, Phys. Rev. Lett. 83 (1999) 4345.
[7] E. Napolitani, D. De Salvador, R. Storti, A. Carnera, S. Mirabella, F. Priolo, Phys. Rev. Lett. 93 (2004) 055901.
[8] D. De Salvador, E. Napolitani, S. Mirabella, G. Bisognin, G. Impellizeri, A. Carnera, F. Priolo, Phys. Rev. Lett. 97 (2006) 255902.
[9] H. Bracht, H.H. Silvestri, I.D. Sharp, E.E. Haller, Phys. Rev. B 75 (2007) 035211.
[10] R. Duffy, V.C. Venezia, A. Heringa, B.J. Pawlak, M.J.P. Hopstaken, G.C.J. Maas, Y. Tamminga, T. Dao, F. Roozeboom, L. Pelaz, Appl. Phys. Lett. 84 (2004) 4283.
[11] V.C. Venezia, R. Duffy a, L. Pelaz b, M.J.P. Hopstaken, G.C.J. Maasc, T. Daoc, Y. Tammingac, P. Graat, Mater. Sci. Eng. B 124 (2005) 245.
[12] D. De Salvador, G. Bisognin, M. Di Marino, E. Napolitani, A. Carnera, H. Graoui, M.A. Foad, F. Boscherini, S. Mirabella, Appl. Phys. Lett. 89 (2006) 241901.
[13] D. De Salvador, G. Bisognin, M. Di Marino, E. Napolitani, A. Carnera, S. Mirabella, E. Pecora, E. Bruno, F. Priolo, H. Graoui, M.A. Foad, F. Boscherini, J. Vac. Sci. Technol. B 26 (2008) 382.
[14] S. Mirabella, D. De Salvador, E. Bruno, E. Napolitani, E.F. Pecora, S. Boninelli, F. Priolo, Phys. Rev. Lett. 100 (2008) 155901.
[15] S.T. Pantelides, Phys. Rev. Lett. 57 (1986) 2979;
P.C. Kelires, J. Tersoff, Phys. Rev. Lett. 61 (1988) 562.
[16] N. Bernstein, J.L. Feldman, M. Fornari, Phys. Rev. B 74 (2006) 205202.
[17] S. Roorda, S. Doorn, W.C. Sinke, P.M.L.O. Scholte, E. van Loenen, Phys. Rev. Lett. 62 (1989) 880;
S. Roorda, et al., Appl. Phys. Lett. 56 (1990) 2097.
[18] E. Napolitani, D. De Salvador, M. Pesce, A. Carnera, S. Mirabella, F. Priolo, J. Vac. Sci. Technol. B 24 (2006) 394.
[19] S. Mirabella, A. Coati, D. De Salvador, E. Napolitani, A. Mattoni, G. Bisognin, M. Berti, A. Carnera, A.V. Drigo, S. Scalese, S. Pulvirenti, A. Terrasi, F. Priolo, Phys. Rev. B 65 (2002) 045209.
[20] F.J. Morin, J.P. Maita, Phys. Rev. 96 (1954) 28.
[21] B.R. Fair, P.N. Pappas, J. Electrochem. Soc. 122 (1975) 1241.
[22] A. Mattoni, L. Colombo, Phys. Rev. B 69 (2004) 45204.
[23] P.A. Stolk, F.W. Saris, A.J.M. Berntsen, W.F. Vanderweg, L.T. Sealy, R.C. Barklie, G. Krotz, G. Muller, J. Appl. Phys. 75 (1994) 7266.
[24] S. Mirabella, D. De Salvador, E. Napolitani, E. Bruno, G. Impellizzeri, G. Bisognin, E.F. Pecora, A. Carnera, F. Priolo, Mater. Res. Soc. Symp. Proc. 1070 (2008), 1070-E05-01.
[25] G. Muller, et al., Phyl. Mag. B 73 (1996) 245;
G. Muller, Curr. Opin. Sol. State Mater. Sci. 3 (1998) 364.
[26] M. Tang, L. Colombo, J. Zhu, T. Diaz de la Rubia, Phys. Rev. B 55 (1997) 14279.